Shock Wave Structure in Polyurethane Foam*

Hideki ONODERA** and Kazuyoshi TAKAYAMA***

Shock wave propagation in polyurethane (PU(R)) foam was experimentally studied. The experiment was conducted in a shock tube by measuring pressure along the PU(R) foam in a shock tube, by means of holographic interferometry and streak camera recording. It was found that the stress-strain curve of PU(R) has an inflection point. When the pressure behind the incident shock wave was below the inflection-point pressure P_c, the wave impedance ratio of the incident shock wave and transmitted pressure wave Z_i/Z_t increased sharply. This indicates that only a small amount of energy is transmitted into the foam if the pressure is below P_c. For pressures larger than P_c, Z_i/Z_t decreases asymptotically to a small finite value.

Key Words: Polyurethane Foam, Compressive Wave, Wave Impedance, Retrograde Material, Dispersive Wave

1. Introduction

Recently, there has been a growing interest in shock wave propagation in multiphase media (i.e., solid-gas[1] or gas-liquid[2] suspensions).

In the case of gas-liquid suspensions, condensation of vapor by shock wave transmission and the existence of expansion shock waves were observed[3]. In the case of solid-gas suspensions, especially in dusty gas shock tube flow, relaxation of particle velocity and particle number density behind the shock wave were studied[1]. In the field of powder metallurgy, shock waves are used for powder compaction[4]. Consequently, it is important to determine the behavior of shock waves in multiphase media.

Recently, shock wave propagation in plastic foam has been the subject of interest, and has been studied experimentally and theoretically[5]-[7]. Weak shock wave propagation in foam located at the end of a shock tube was studied theoretically by Sano[8]. Pressure measurements of shock wave propagation in long pieces of foam were reported by Henderson et al.[9] Generally speaking, when a shock wave collides with foam, it is attenuated. Therefore, the foam may be used as a shock wave attenuator. However, at present there is no reliable model capable of describing the properties of foam behind a shock wave.

It is the purpose of the present paper to report the results of careful investigation of shock wave propagation in foam using pressure measurement and flow visualization (streak and double-exposure holographic interferometry). From the obtained results, the wave propagation, its structure and the wave stability will be discussed. Finally, pressure wave propagation in foam is examined from the view point of wave impedance.

2. Nomenclature

a : Velocity of sound m/s
E : Young's modulus MPa
M : Mach number
P : Pressure kPa
P_c : Pressure at the inflection point of stress-

* Received 29th September, 1992. Paper No. 91-0628B
** Department of Mechanical Engineering, Iwate University, 4-3-5 Ueda, Morioka 020, Japan
*** Institute of Fluid Science, Tohoku University, 2-1-1 Katahira, Aoba-ku, Sendai 980, Japan

strain curve kPa
u : Particle velocity m/s
T : Power transmission coefficient
Z : Wave impedance kg/(m^{2}s)
ε : Strain
ξ : Inverse shock strength $=P_0/P_i=(7M^2-1)/6$
σ : Stress MPa
ρ : Density of PU(R) kg/m^3
subscripts
i : incident
t : transmitted

3. Experimental Apparatus

Experiments were conducted in the shock tube of the Shock Wave Research Center, Institute of Fluid Science, Tohoku University. The shock tube has a low-pressure channel of 60 mm×150 mm cross section. The driver chamber has a diameter of 150 mm and is 1.5 m long. The test gas was air and pressure ranging from 0.065 to 0.1 MPa. The driver gas was nitrogen. Mylar diaphragms of 3 μm to 188 μm thick were used for obtaining the required incident shock wave Mach number ranging from 1.04 to 1.42. Good repeatability was obtained.

Foam pieces having either 25 mm or 400 mm length were inserted inside the shock tube, in contact with the shock tube wall. Pressure distribution was measured at the upper wall of the shock tube along the interface with the foam. Nine pressure transducers (Kistlar 603B) were mounted at the upper shock tube wall as shown in Fig. 1(b). Pressure history records were stored using wave memory (Asuno-giken AS-1000) and analyzed by with a personal computer (NEC PC9801VX).

For flow visualization, double-exposure holographic interferometry was used. The system employed a ruby laser (Apollo Lasers Inc., 22HD, 25 ns pulse width and 2 J/pulse output) as a light source and streak photographs were taken using an image-converter camera (Hadland Photonics, IMACON 790) with an agron-ion laser (Spectra Physics 2030, 6 W output) as a light source.

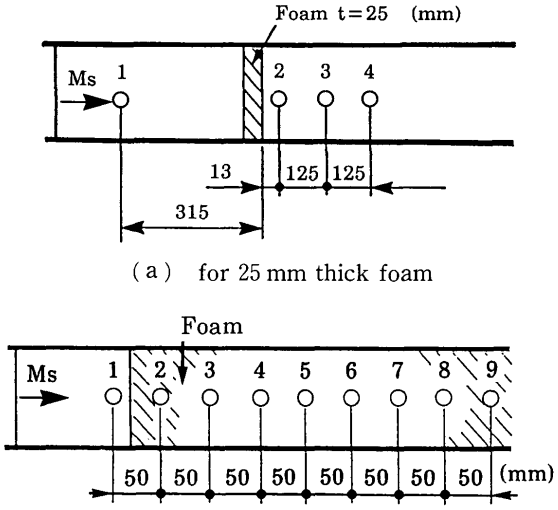

(a) for 25 mm thick foam

(b) for 400 mm thick foam

Fig. 1 Pressure transducers arrangement

4. Material Testing

Open cell type rigid polyurethane foam (PU(R)) was used in the present experiments. It have 60 mm× 150 mm cross section and 25 mm or 400 mm length. The foam was inserted inside the shock tube filling the space it will occupied, i.e., creating a uniaxial stress condition. The stress-strain relation of the investigated foam was measured using a material testing machine (Shimazu Testing Machine, Auto-Graph AG5000-C). This machine enables control of the compression speed. Typical stress-strain curves obtained for 50 mm-long foam and compression speed of 50 mm/min are shown in Fig. 2. The dashed line represents the results of uniaxial stress loading under unconstrained conditions, while the solid line represents values obtained under lateral constraint, which was the actual compression mode during the experimental study. The compression speed of material testing is not the same as that in shock tube experiments; however, we can obtain useful reference data from this figure. This stress-strain curve simply increases in the case of unconstrained. On the other hand, in the lateral constraint case for relatively low stress, strain simply increases; however, when the strain exceeds a certain value, the curve becomes negative. Mechanical properties of the present material are listed in Table 1.

5. Results and Discussion

The inflection point stress P_c of the stress-strain curve under lateral constraint is 9.6 kPa (with 150 mm

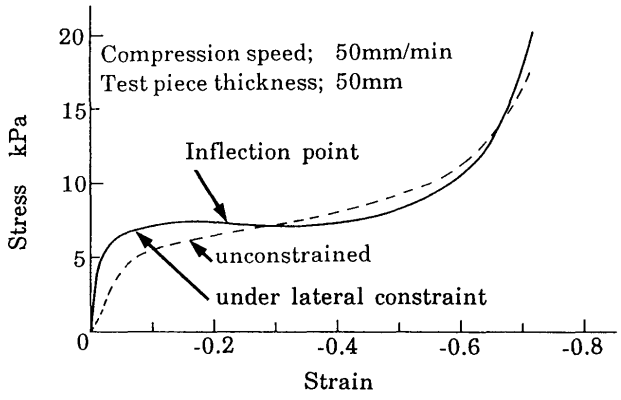

Fig. 2 Stress-strain curves of the foam in study

foam length and 500 mm/min compression speed). If we assume that this stress is comparable to the pressure acting on the foam, we can calculate the equivalent shock wave Mach number to be $M_s=1.04$.

Figure 3 shows the pressure history and flow visualization for 25 mm-thick foam at $M_s=1.04$. In Fig. 3(a) pressure measurements recorded by the transducers, arranged as in Fig. 1(a) are shown. The shock wave which emerges from the thin foam is significantly attenuated, so much so that no discontinuity is present; instead we see a dispersed pressure wave. In this case, the pressure wave speed is about 250 m/s. The peak pressure of the transmitted compression wave is higher than the pressure obtained behind the incident wave. This is evident, since the pressure behind the reflected wave is always higher than that behind the incident wave. This high-pressure region emerges from the foam. As time proceeds, the wave is gradually attenuated. Foam is useful for shock wave attenuation except for the case in which it is supported at its rear surface by a rigid wall. Figure 3(b) is the corresponding streak photograph taken through a 0.5 mm-wide slit with 0.1 μs/mm streak rate and 100 mm marker distance. The ordinate denotes the length and the abscissa denotes the time. Incident and reflected waves are well resolved and the transmitted pressure wave, A, is clearly seen.

Figure 4 shows the case in which $M_s=1.28$. The pressure rise through the transmitted wave gradually grows steeper. Finally, at location 4, the pressure wave transforms into a discontinuous pressure change, i.e., it becomes a shock wave again. At location 2 we can see a two-step pressure rise in the transmitted wave. One step is the transmitted incident pressure wave and the other is the transmitted high-pressure region behind the wave reflected from the foam leading edge. Because of differences in the corresponding speed of sound in the foam, the continuous pressure distribution becomes these two pressure waves, shown as two steps. At location 2, the second stage of the pressure rise is 1.3 times higher than the pressure behind the reflected wave. The speed of the compression wave B from location 2 to 3 is about 100 m/s, and that of compression wave A from 2 to 3 is about 310 m/s. As the wave travels from location 3 to 4, it disperses. Figure 4(b) shows a streak camera recording under the same conditions as in Fig. 4(a). The two-step pressure rise, i.e., transmitted pressure wave A and pressure wave B corresponding to the second stage of the pressure rise, is clearly seen in Fig. 4(b).

As mentioned before, the incident shock wave Mach number comparable to the inflection point stress is 1.04. However, we can now say that the wave propagates completely differntly at pressure P_c when we take into account differences in compression speed and foam length between thematerial testing and in the shock tube experiment.

Table 1 Mechanical properties of the PU(R) foam in study

Density	31.5±5 kg/m³ (Spatial) 1100 kg/m³ (Material)
Young's Modulus	0.134 MPa
Velocity of Sound	65.7 m/s

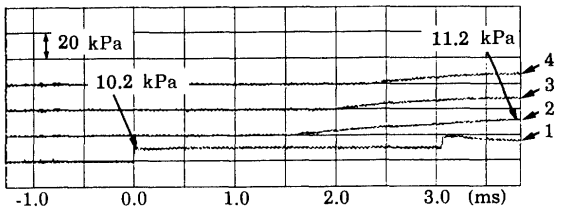

(a) Pressure measurement (numbers on the right correspond to the pressure transducers shown in Fig. 1(a))

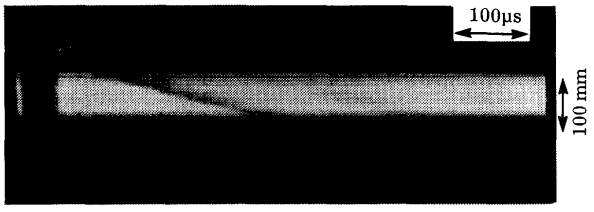

(b) streak recording

Fig. 3 Shock wave propagation over PU(R) foam, $M_s=1.04$

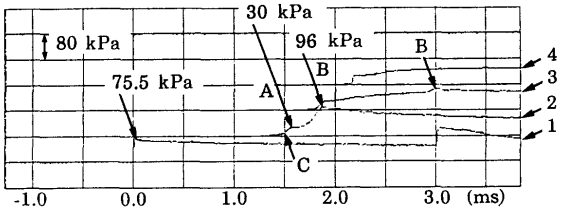

(a) pressure measurement (Numbers on the right correspond to the pressure transducers shown in Fig. 1(a))

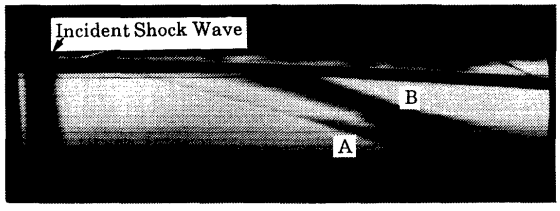

(b) streak recording

Fig. 4 Shock wave propagation over PU(R) foam, $M_s=1.28$

In Fig. 5 the foam end displacement for a 100 mm-long piece of foam caused by collision with the incident shock wave is shown; these results were deduced from streak photograph records. The incident shock wave Mach numbers were 1.08, 1.18, 1.28 and 1.41. For each Mach number, the leading edge of the foam accelerated just after the collision and the displacement velocity become constant at about 100 μs after that. The gradient of the solid line denote the mean velocity of loading edge displacement for corresponding incident shock waves.

Figure 6 presents these results as a function of ξ and the foam displacement velocity. When $\xi > 0.8 (M_s = 1.1)$, the mean velocity is relatively small, whereas when $\xi < 0.8$, the mean velocity increases rapidly.

The pressure distribution along the foam was measured using pressure transducers employing the arrangement shown in Fig. 1(b). The results, taken at 400 μs intervals are shown in Fig. 7. In this figure the absissa indicates the pressure gauge number and the ordinate is the pressure ratio. The interval between neighboring pressure gauges is 50 mm. The solid lines are curve fittings to the measured pressure values. Figure 7(a) shows the results obtained for $M_s = 1.04$. From the results shown in Fig. 5, the foam displacement obtained 2.8 ms after shock wave collision (correspond to 7th curve in Fig. 7(a)) is about 10 mm.

The foam/air interface is a kind of contact surface discontinuity ; therefore there is no pressure difference across this interface. In the case of $M_s = 1.04$, the leading transmitted pressure wave A propagates in the foam; however, pressure wave B, which propagates in the foam at the speed of sound, is attenuated since the speed of sound decreases as Young's modulus decreases[11]. As a result the wave speed of B is only about 1.7 m/s.

Consequently, for this range of Mach number, the transmitted pressure wave in the foam is never transformed into a discontinuity and it cannot retain its shape. For $P < P_c$, the pressure wave in the foam is not stable. Figure 7(b) shows the results obtained for $M_s = 1.28$. The foam displacement at 4 ms after collision with the incident shock wave (corresponding to the 10th curve in Fig. 7(b)) is about 230 mm. In

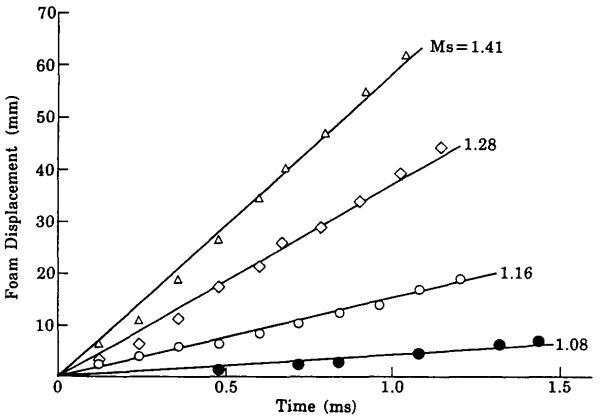

Fig. 5 Displacement of the front edge of the foam for different incident shock Mach numbers

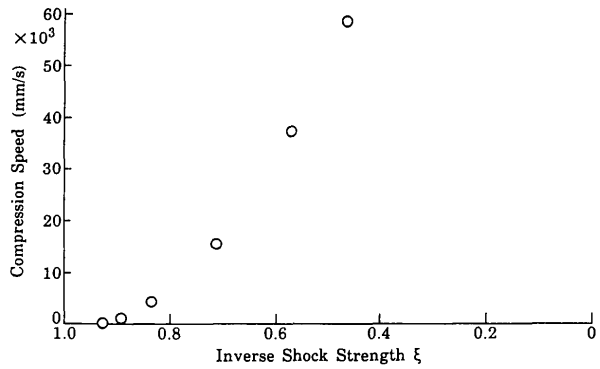

Fig. 6 Dependence of the leading edge velocity of the foam on the inverse shock strength

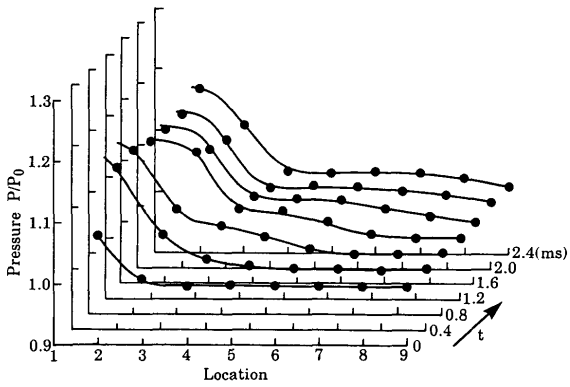

(a) $M_s = 1.04$

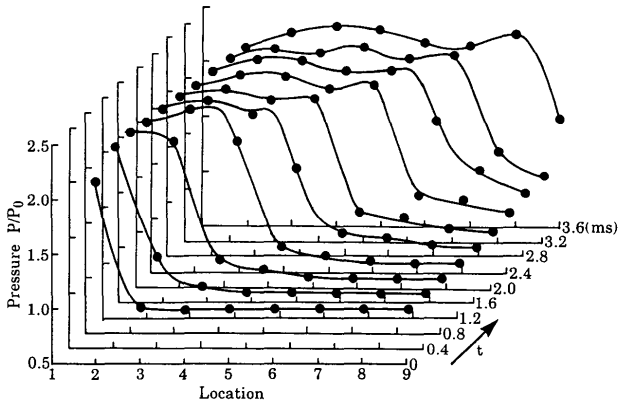

(b) $M_s = 1.28$

Fig. 7 Pressure distribution inside the foam at different times (numbers along the abscissa correspond to the location of the pressure transducers shown in Fig. 1(b))

this situation, only the pressure transducers in locations 5 to 9 can measure pressure in the foam. However, as mentioned before, there is no pressure difference across the foam/air interface. If we observe the transmitted wavefront, it becomes apparent that the foam displacement does not influence the pressure measurement. In this range of Mach number ($P>P_c$), similar to the case of $M_s=1.04$, the transmitted wave propagates in the foam and the high-pressure region which follows the wave retains its shape. In this case, the pressure wave in the foam is stable. From these conclusions, we can describe the mechanism of the two-stage pressure rise shown in Fig. 4 as an initial dispersed wave followed by a high-pressure region. Significant foam displacement induced by the shock wave collision makes the pressure behind the shock wave front less than the pressure for rigid wall head-on collision. When the high-pressure region is transmitted through the foam, the expansion wave catches up to the high-pressure region and the pressure decreases rapidly.

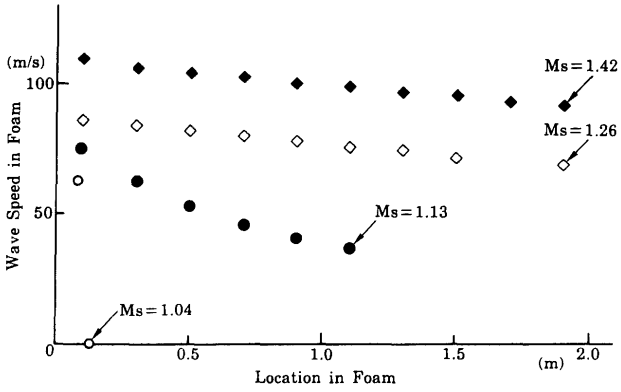

Fig. 8 Dependence of the wave velocity on its propagation distance inside the foam

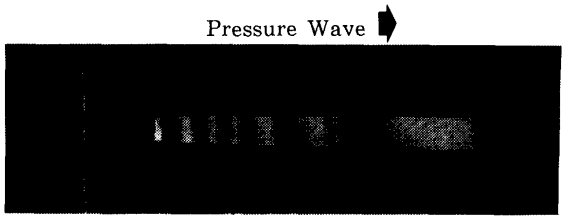

(a) holographic interferogram

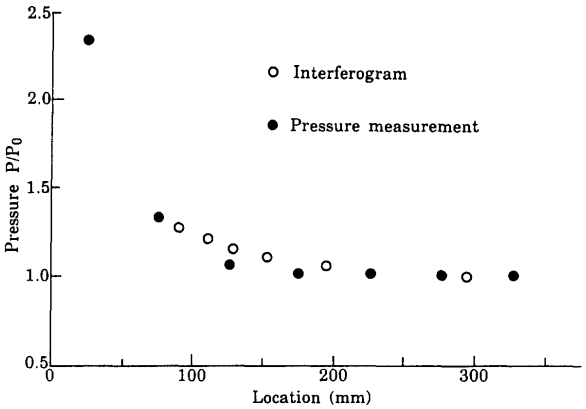

(b) obtained from pressure and optical measurements

Fig. 9 Pressure distribution inside the foam

Figure 8 shows the shock wave propagation in the foam, where the ordinate is the wave speed and the absissa indicates the location. For the case in which $\xi<0.8$, the wave is transmitted with a slight velocity decrease; however, in the case of $\xi>0.8$, the wave velocity in the high-pressure region becomes very low. Consequently, the transmission properties in the foam are completely different beyond the border value of $\xi=0.8(M_s=1.1)$.

Figure 9(a) shows a holographic interferogram of pressure wave propagation in the slitted area of the foam (the foam was cut to 20 mm width×250 mm length). Fringes in this picture correspond to isopycnics. In this figure, the density change corresponding to one fringe shift is about 3.8% of the original density[12]. If we assume that the flow field is isentropic, we can calculate the pressure ratio from this value. In this case, the pressure difference corresponding to one fringe shift is about 5.3% of original pressure. A comparison between pressures deduced from the interferogram and those measured with Kistler gauges is shown in Fig. 9(b). Pressure deduced from interferograms is the pressure of the air part, i.e., at the slit of the foam, whereas pressure measured with the Kistler gauges is the pressure in the foam. However, the difference between these two is no more than 11%.

In spite of the fact that the pressure induced by the reflected shock wave on the foam leading edge, P_{2pur}, increases as the incident shock wave Mach number increases, its value is smaller than the pressure that would have been obtained had the incident thock wave been reflected head-on from a solid surface P_{2solid}. The ratio between these pressures, P_{2pur}/P_{2solid}, as a function of the inverse shock strength across the incident shock wave is shown in Fig. 10. It is clearly seen from this figure that the higher the incident shock wave Mach number, the greater the attenuation of the initial head-on reflected pressure. When $\xi>0.8$, the pressure ratio is almost equal to unity, which is almost the same as the result of a head-on reflection from a rigid wall.

Consequently, for the foam in study, the value $\xi=0.8(M_s=1.1)$ acts as a divider of interaction properties of foam with shock waves.

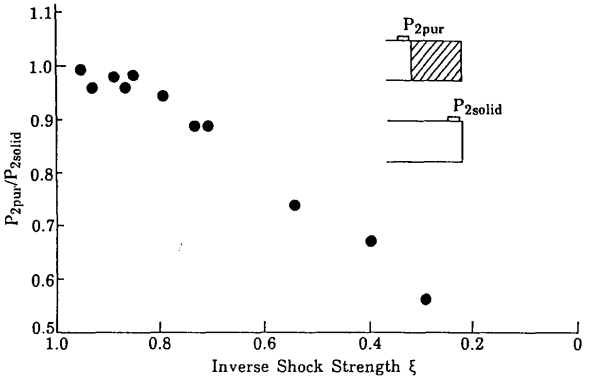

Fig. 10 Relative reduction of the initial pressure at the leading edge of the foam with inverse shock strength

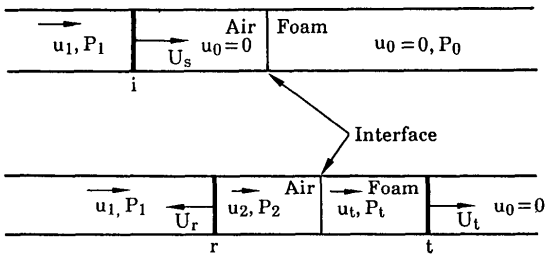

Fig. 11 Definition of flow regions and flow parameters

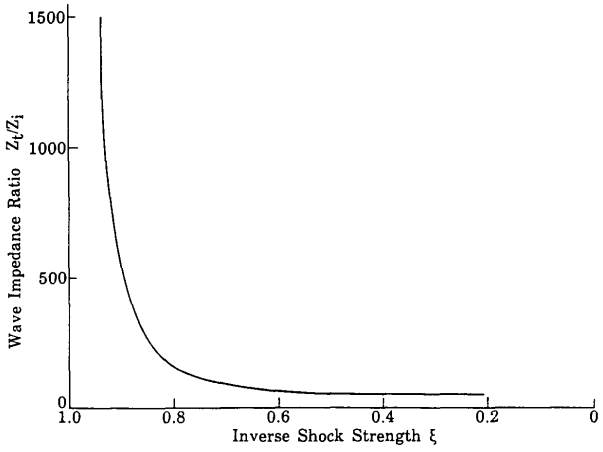

Fig. 12 Dependence of the wave impedance ratio on the inverse shock strength across the incident shock wave

6. Wave Impedance

When several pressure pulses are applied to a medium, they induce particle velocity in it; wave impedance is defined as the ratio of this particle velocity and the pressure difference[10]. The wave impedance value is equal to acoustic impedance when the Mach number is nearly unity and the particle velocity is comparatively small. Wave impedances Z_i and Z_t are defined in terms of the variables presented in Fig. 11 as

$$Z_i \equiv \frac{P_i - P_0}{u_i - u_0},\ Z_t \equiv \frac{P_t - P_0}{u_t - u_0} \quad (1)$$

The power transmission coefficient T_t is defined as

$$T_t \equiv \left| \frac{(P_t - P_0)^2 Z_i}{(P_i - P_0)^2 Z_t} \right| \quad (2)$$

Foam displacement speed is obtained as function of the Mach number. Assuming that the foam displacement velocity is equal to the particle velocity, and that, the pressure wave in the foam can be treated as a discontinuity, we can calculate the foam's wave impedance.

Figure 12 shows the wave impedance distribution as function of the inverse shock strength. It is evident from this figure that as ξ exceeds 0.8, the ratio Z_t/Z_i approaches infinity, which means that T_t approaches zero. In other words, when the incident shock wave is weak, the transmitted wave decays quickly and the energy difference across it vanishes. The opposite happens in the case of a moderate incident shock wave ($\xi < 0.7$, i. e., $M_s > 1.17$ as seen in Fig. 12). In this case, the ratio Z_t/Z_i reaches a finite value, which in turn results in an energy change across the transmitted wave with a finite non-zero value. In such a case, the attenuation is nearly zero.

As shown in Fig. 7, the $M_s = 1.28$ shock wave is stable in foam, and when $M_s = 1.04$, only a dispersed wave travels in the foam, whereas a high-pressure region stagnates in the foam. Now we can say that the value $\xi = 0.8$ (inflection point of the stress-strain curve) acts as a phase-change point.

When $Z_i > Z_t$, the reflected wave is an expansion wave, but for $Z_i < Z_t$ it becomes a compression wave[11]. From this point of view, in the present experiments the reflected wave is always a compression wave. Consequently, we can predict the behavior of pressure waves in foam by checking the wave impedance.

7. Conclusion

The head-on collision of a planar shock wave with piece of open cell foam has been investigated using pressure measurement and flow visualization techniques (holographic interferometry and streak recording). The results are summarized as follows.

(1) A pressure wave in foam is stable when $P > P_c$ and unstable when $P < P_c$, where P_c denotes the inflection point pressure in the foam stress-strain curve.

(2) When $P < P_c$, the pressure ratio P_{2pur}/P_{2solid} is almost equal to unity and foam acts like a rigid wall. When $P > P_c$, foam end displacement influences the results.

(3) To resolve the wave behavior in foam, a

modified wave impedance concept is adopted. When $P<P_c$, the wave impedance ratio Z_t/Z_i increases rapidly. On the other hand, in the case of $P>P_c$, Z_t/Z_i attains a small finite value. This means that when $P<P_c$, the energy difference across the air / foam interface vanishes and it is difficult for the high-pressure region to enter into the foam.

Acknowledgements

The authors would like to express their gratitude to Messrs. O. Onodera, H. Ojima and K. Takahashi of the Institute of Fluid Science, Tohoku University for their assistance in conducting the present experiments. The authors are also indebted to Messrs. T. Sato and M. Nakai of the Miyagi Prefectural Laboratory for Industry for their assistance in conducting the measurement of foam properties.

References

(1) Sugiyama, H., Takayama, K., Shirota, T. and Doi, H., Shock wave induced flow past a circular cylinder in a dusty-gas shock tube, Trans. Jpn. Soc. Mech. Eng. (in Japanese) Vol. 53, No. 496, B (1987), p. 3533.

(2) Thompson, P. A. and Kim, Y. G., Direct observation of shock splitting in a vapour ; liquid system, Phys. Fluids, Vol. 26, No. 11 (1983), p. 3211.

(3) Borisov, A. A., Borisov, AL. A., Kutateladze, S. S. and Nakoryakov, V. E., Reafaction shock wave near the critical liquid-vapour point, J. Fluid Mech., Vol. 126 (1983), p. 59.

(4) Sano, Y., Miyagi, K. and Tokushima, K., Dynamic equilibrium constitutive relations of copper powder within dies subjected to multiple shock compactions, Trans. ASME, J. Eng. Mat. Tech., Vol. 111 (1989), p. 183.

(5) Onodera, H., Shock wave propagation in polyurethane foam, Prepr. of Jpn. Soc. Mech. Eng., (in Japanese) No. 900-14 (1990), p. 186.

(6) Onodera, H., Shock wave propagation in polyurethane foam (2nd report), Prepr. of Jpn. Soc. Mech. Eng., (in Japanese) No. 900-59 (1990), p. 198.

(7) Onodera, H. and Takayama, K., Shock wave structure in polyurethane foam, Proc. Nat. Symp. Shock Waves (in Japanese) (1990), p. 257.

(8) Sano, Y., Qualitative analysis of degradation processes of attenuating plane waves by undetermined system theory, J. Appl. Phys., Vol. 67, No. 9 (1990) p. 4072.

(9) Henderson, L. F., Virgona, R. J., Di, J. and Gvozdeava, L. G., Refraction of a normal shock wave from nitrogen into polyurethane foam, personal communication (1990).

(10) Henderson, L. F., On the refraction of shock waves, J. Fluid Mech. Vol. 198 (1989), p. 365.

(11) Tokuoka, T., Wave Mechanics, (in Japanese) (1989), p. 111, Saiensu-sya.

(12) Takayama, K. and Watanabe, W., Shock wave diffraction around the concave wall, Rep. Inst. High Speed Mech., Tohoku Univ., (in Japanese) Vol. 45, No. 398 (1980), p. 33.